

Effective tuning of the charge state of a single InAs/GaAs quantum dot by an external magnetic field

E. S. Moskalenko,^{1,2} L. A. Larsson,¹ M. Larsson,¹ P. O. Holtz,¹ W. V. Schoenfeld,³ and P. M. Petroff³

¹*IFM Material Physics, Linköping University, S-581 83 Linköping, Sweden*

²*A. F. Ioffe Physical-Technical Institute, Russian Academy of Sciences, 194021, Polytechnicheskaya 26, St. Petersburg, Russia*

³*Materials Department, University of California, Santa Barbara, California 93106, USA*

(Received 14 April 2008; revised manuscript received 1 July 2008; published 6 August 2008)

A microphotoluminescence study of single InAs/GaAs quantum dots (QDs) in the presence of an applied external magnetic field is presented. Attention is focused on the redistribution between the spectral lines of a single QD observed at increasing magnetic field parallel to the growth direction (Faraday geometry). The redistribution effect is explained by considering the electron drift velocity in the QD plane that affects the probability for capture into the QD. In contrast, no redistribution is observed when applying the magnetic field perpendicular to the growth direction (Voigt geometry).

DOI: [10.1103/PhysRevB.78.075306](https://doi.org/10.1103/PhysRevB.78.075306)

PACS number(s): 73.21.La, 73.63.Kv, 78.67.Hc, 71.35.Pq

I. INTRODUCTION

Quantum dots (QDs) are widely considered as perspective candidates for various optoelectronic applications such as QD lasers,¹ QD memory devices,² and single-electron transistors.³ However, any operation of the QD-based devices is considerably affected by excess charge (electrons e 's or holes h 's) stored inside the QD,^{2,3} which highlights the importance to practically control the charging or discharging of QDs. Several experimental approaches^{4–15} have been employed to load QDs with extra charges. However, a sophisticated sample design,⁴ a definite level of intentional doping,⁵ or an impurity background doping in the surrounding barriers⁶ were required. An applied external voltage was used in samples containing an n -doped layer with contacts^{8–10} or in samples prepared as Schottky diodes^{11–15} to create extra e 's or h 's inside the QDs. It is important to note that the applied voltage may deform the e 's and h 's wave functions, which could result in the change of their interaction energies; a fact which has been suggested to be the reason for deviations between the calculated interaction energies and the experimentally derived energies.¹⁶

In the present paper, we apply an external magnetic field, which facilitates an effective control of the charge configuration in an individual QD and, consequently, its optical properties by pure optical means. An external magnetic field has been frequently applied in single QD spectroscopy in the past decade.^{10,12–15,17–21} To access individual QDs, submicron diameter apertures in a metal mask were patterned on the sample surface^{13,17} or rather small ($\sim 100\div 200$ nm) mesas^{10,14,18–21} were fabricated. As a result, the carrier spin dynamics has been revealed^{13,15,20} and detailed information on the exciton fine structure in individual QDs of InAs,^{18,19,21} GaAs,^{15,17} InP,¹⁰ and CdSe (Ref. 20) has been obtained. However, in all these studies with an external magnetic field, an important step of carrier dynamics was inevitably overlooked—carrier transport in the barriers and/or in the wetting layer (WL)—on which QDs are normally grown prior to capture into the QDs. The importance of the latter originates from the fact that in most of the optical experiments with QDs, carriers are primarily generated somewhere outside the QDs in the sample (e.g., in the barriers or in the WL).

In our earlier study, ensembles of QDs were investigated by means of conventional photoluminescence (PL) in the presence of a magnetic field up to 14 T for samples with different QD density.²² In our present investigation, we have used microphotoluminescence (μ -PL) of a sample with a rather low QD density (the averaged interdot distance is ≈ 10 nm), allowing us a direct optical access to an individual QD without arranging apertures or mesas, which considerably restrict the area of the sample (around the QD under study) excited by the laser beam. Consequently, in our experimental conditions, a laser beam was focused on the sample surface down to a spot diameter of 2 μ m (still considerably larger than the lateral size of the single QD of 35 nm). Thanks to this experimental approach, we observed that the external magnetic field (B) applied in Faraday geometry (i.e., perpendicular to the sample surface) affects the motion of e 's and h 's differently in the plane of the sample prior to capture into the QD. This is reflected in our experiments as changes (decrease) in the extra negative charge accumulated in the QD at $B=0$.

To explain the observed phenomenon, a model is developed according to which the lateral motion of e 's is slowed down by B considerably more than for h 's (due to the fact that the cyclotron frequency for e 's is higher than for h 's in the GaAs barriers). This increases the probability for e 's to become captured into localizing potentials (positioned at the GaAs/WL boundary) on their way toward the QD and, accordingly, effectively decreasing the electron flux while the flux of h 's is almost left unaffected. The strength of this effect, being highest at helium temperatures, is progressively reduced as the sample temperature increases due to thermal ionization of trapped e 's out of the localizing potentials.

Complementary studies in Voigt geometry (i.e., B is applied parallel to the sample plane) show almost no effect of B on the charge state of a QD. Consequently, the magnetic field does not quantize the in-plane motion of photoexcited carriers in this geometry. It should be stressed that our findings could be widely used in practice as an effective tool to control the charge state of QD-based devices.

II. SAMPLE AND EXPERIMENTAL SETUP

The sample studied was grown by molecular beam epitaxy (MBE) on a semi-insulating GaAs (100) substrate. The

buffer layer was prepared with a short-period superlattice 40×2 nm/2 nm AlAs/GaAs at a growth temperature of 630 °C. On top of a 100 nm GaAs layer, the QDs were formed from a 1.7-monolayer (ML)-thick InAs layer deposited at 530 °C. A first growth interruption of 30 s was used to improve the size distribution. Then the dots were covered with a thin GaAs cap layer with a thickness of $t_{\text{cap}}=3$ nm before a crucial second growth interruption of 30 s. Finally, a 100-nm-thick GaAs layer was deposited to protect the QDs. As a result, lens-shaped InAs QDs were developed with the height and diameter of 4.5 and 35 nm, respectively. The dot density was low with an average distance between the adjacent QDs of around 10 μm , which allowed excitation of a single QD in a diffraction-limited $\mu\text{-PL}$ setup.

To excite the sample, we used a Ti:Sapphire laser, where the beam was focused on the sample surface down to a spot diameter of 2 μm . The excitation energy of the laser ($h\nu_{\text{ex}}$) was tuned in the range from 1.23 to 1.77 eV with a maximum excitation power (P_0) of 200 μW . For dual-laser excitation conditions, a semiconductor laser operating at a fixed excitation energy of 1.589 eV with a maximum power output of 200 nW was used as the principal excitation source, while a Ti:Sapphire laser was used as an infrared laser operating at a fixed excitation energy $h\nu_{\text{IR}}=1.23$ eV with a maximum excitation power (P_{IR}) of 100 μW . The sample was positioned inside a continuous-flow cryostat, which allowed temperature (T) to change from 3.8 up to 100 K.

The luminescence signal passed through the retarder (used as a quarter-wave plate) combined with a Glan-Thomson linear polarizer and was further dispersed by a single-grating 0.55-m monochromator combined with a nitrogen cooled CCD camera that allows a spectral resolution of 0.1 meV. The sample was inserted in the center of a superconducting magnet of solenoid type. A magnetic field (B) up to 5 T was applied in Faraday or Voigt geometry with respect to the plane of the sample.

Seven single dots at different spatial positions were examined with a resulting analogous behavior. For consistency, we present the results taken from only one single QD to demonstrate the typical behavior of QDs in the present study.

III. EXPERIMENTAL RESULTS AND DISCUSSION

Figure 1 shows low-temperature ($T=4.2$ K) $\mu\text{-PL}$ spectra of an individual QD measured at an excitation energy ($h\nu_{\text{ex}}$) above the GaAs barrier ($E_{\text{GaAs}}=1.518$ eV) and at different values of the magnetic field (applied in Faraday geometry) as indicated in the figure. The excitation light was linearly polarized and the emission was analyzed with respect to its circular polarization σ^- (σ^+) shown in Fig. 1 by dotted (solid) lines. It is seen that altogether three emission lines marked as X^0 , X^{1-} , and X^{2-} can be registered depending on the exact value of B . These lines were identified in our previous work²³ as neutral, singly, and doubly negatively charged exciton complexes, i.e., these lines are detected in $\mu\text{-PL}$ spectra when charge configuration of a QD at the emission event consists of $1e1h$, $2e1h$, and $3e1h$, respectively.

The effect of the accumulation of the extra e 's in the QD (at $B=0$) was shown²³ to be crucially dependent on the exact

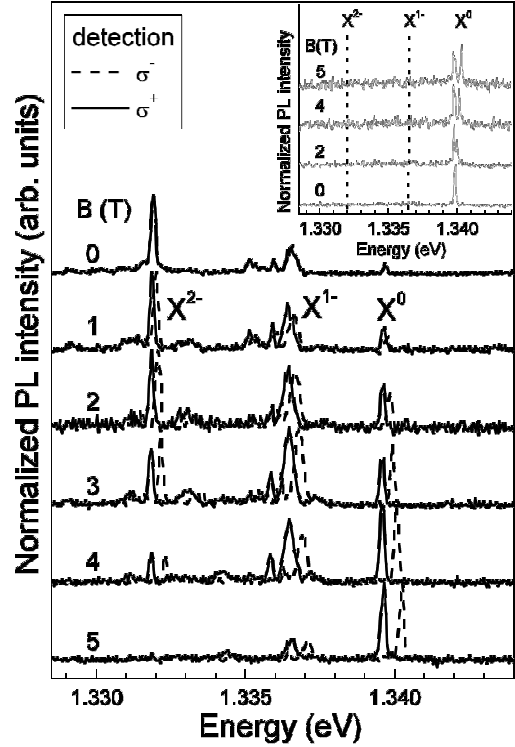


FIG. 1. $\mu\text{-PL}$ spectra of an individual QD recorded at $T = 4.2$ K, $h\nu_{\text{ex}}=1.540$ eV, $P_0=20$ nW, and for a number of magnetic fields applied in the Faraday geometry are shown by dotted (solid) lines for the detection in the σ^- (σ^+) polarization. The excitation light was linearly polarized. The inset shows $\mu\text{-PL}$ spectra of the same QD measured at $T=4.2$ K, $h\nu_{\text{ex}}=1.430$ eV, $P_0 = 100$ nW, and for a number of magnetic fields.

value of $h\nu_{\text{ex}}$, i.e., on the difference between kinetic energies of an e (E_e) and h (E_h) relative to the bottom of the conduction and top of the valence band of GaAs, respectively. Indeed, at low excitation powers used in the present study (at which Auger processes can be neglected) carriers can release their kinetic energy only by emission of the cascade of acoustic phonons [this is true for the case when E_e (E_h) is less than the optical-phonon energy, i.e., 36.2 meV in the case of GaAs (Ref. 24)]. Consequently, for a higher kinetic energy, a longer time is needed for carriers to cool down to form an exciton and to recombine. As a result, it is predicted that carriers with a longer “cooling” time are more likely (compared to carriers with a shorter cooling time) to approach a QD and become captured into it. At the experimental conditions used presenting this study, ($h\nu_{\text{ex}}=1.540$ eV), the energies $E_e=19.2$ meV and $E_h=2.9$ meV were calculated on the basis of a simple model of band-to-band excitation in direct band-gap semiconductors in the approximation of parabolic valence and conduction bands, which are characterized by the effective masses of $m_e=0.067m_0$ and $m_h=0.45m_0$ (Ref. 24) (where m_0 is the free-electron mass).

It is seen that for an increasing magnetic field, all three lines X^0 , X^{1-} , and X^{2-} exhibit a Zeeman splitting into two oppositely circularly polarized components (Fig. 1). Based on the measured splitting between the σ^- and σ^+ components, we can estimate a g factor; g_{ex} for the neutral exciton $g_{\text{ex}}=-2.2$. This value is consistent with $g_{\text{ex}}=-3$ found by

other authors in samples with InAs/GaAs QDs.²¹ However, the most remarkable effect of the magnetic field on the μ -PL spectra of an individual QD is the redistribution between spectral lines (Fig. 1). Indeed, at $B=0$, the μ -PL spectrum consists essentially of the PL line X^{2-} , which decreases in intensity with increasing B at the expense of the appearance of the X^{1-} and X^0 PL lines to completely vanish at $B=5$ T (Fig. 1). Instead, the X^0 PL line dominates the μ -PL spectrum at these experimental conditions. Consequently, in what follows, we will entirely concentrate on the magnetic-field-induced redistribution and leave the modifications in the fine structure of all three spectral lines as a subject for following studies.

As explained above, the observation of the intensity distribution of the three spectral lines in the PL spectrum shows the charge configuration in the QD. Accordingly, the redistribution of the μ -PL spectra with increasing B (Fig. 1) should be explained in terms of the magnetic-field-induced “neutralization” of the negative charge accumulated in the QD at $B=0$. To obtain further insight into the observed phenomenon, the sample under study was excited with $h\nu_{\text{ex}}=1.430$ eV, which is below the WL band-gap energy (≈ 1.450 eV as determined from PL spectra of the WL), i.e., directly into the QD. At these excitation conditions, no carrier transport in the GaAs barriers or in the InAs WL is possible prior to capture into the QD. The corresponding μ -PL spectra of the same QD measured at excitation with $h\nu_{\text{ex}}=1.430$ eV are shown in the inset in Fig. 1. It is seen that a neutral charge state of the QD at $B=0$ is monitored and no redistribution effect at higher magnetic fields is registered. Consequently, the redistribution effect achieved for excitation with $h\nu_{\text{ex}} > E_{\text{GaAs}}$ (Fig. 1) is explained in terms of magnetic-field-induced changes in the transport of carriers in the GaAs barriers. The major role played by the carrier transport in the processes studied in our sample is further justified by the experimental fact that the spectrally integrated (including all three lines observed) PL intensity of the QD (I_{QD}) is approximately 1% relative to the corresponding intensity of the entire sample, which is to be compared with the corresponding volume ratio of $\approx 10^{-6}$ – 10^{-5} . Consequently, the PL signal from the QD is primarily not determined by the absorbing dot volume but is rather due to transport and capture processes of carriers from the barriers into the QD.

Evidently, our experimental data (Fig. 1) imply that the magnetic field should affect the transport of e 's essentially more than that of h 's. To considerably modify the motion of the carriers, the magnetic field should be rather strong. The usual criterion to evaluate the strength of the magnetic field applied is to compare $\omega_c^{e(h)} \times \tau_{\text{sc}}^{e(h)}$ with unity.²⁵ Here $\omega_c^{e(h)} = e^*B/m_{e(h)}$ is the cyclotron frequency, where e^* is the elementary charge, $m_{e(h)}$ and $\tau_{\text{sc}}^{e(h)}$ are the effective mass and scattering time of an electron (hole), respectively. A magnetic field is considered to be strong if $\omega_c^{e(h)} \times \tau_{\text{sc}}^{e(h)} > 1$ because when forming the cyclotron orbit, it is required that a carrier should be able to accomplish at least one turn along the orbit before it is scattered. The value of $\hbar\omega_c^{e(h)}$ achieved at $B=5$ T for the electron and for the hole is calculated to be $\hbar\omega_c^e=8.7$ meV and $\hbar\omega_c^h=1.3$ meV, respectively. Typical value of scattering time τ_{sc}^e (τ_{sc}^h) for an $e(h)$ can be calculated from the carrier mobility ($\mu^{e(h)}$) according to the equation

$\mu^{e(h)} = e^* \tau_{\text{sc}}^{e(h)} / m_{e(h)}$. The carrier mobility of e 's (h 's) in high quality GaAs material was experimentally studied in Ref. 26 (Ref. 27) for a wide range of sample temperatures (T). Accordingly, for $T=4.2$ K (the case of the present study), the scattering time is calculated to be $\tau_{\text{sc}}^e=3.40$ ps and $\tau_{\text{sc}}^h=0.74$ ps, respectively.²⁸ We finally find $\omega_c^e \times \tau_{\text{sc}}^e=8.9$ and $\omega_c^h \times \tau_{\text{sc}}^h=0.29$ at $B=5$ T. It is then clear that a magnetic field of 5 T is still too small to affect the motion of the holes, while already at $B=1$ T, the kinetic energy of the electrons could be assumed to become quantized in units of $\hbar\omega_c^e$ (i.e., Landau levels are formed). Thus, we will consider the hole motion to be almost unaffected by the magnetic field and will concentrate on the possible mechanisms for which a magnetic field could influence the electron flux.

To get an insight into the carrier motion, we note first that photoexcited carriers, which migrate in the plane of the GaAs barriers (or/and the WL) prior to capture into the QD, will (with a certain probability) become localized at potential fluctuations at the GaAs/WL interface, which are due to the growth-induced variations of alloy composition and strain along the plane of the WL.^{29–31} The density of these localizing potentials [two-dimensional (2D) islands or clusters³⁰] was found to depend on the number of InAs MLs deposited during the growth procedure. In particular, for the case of 1.7 ML deposition, (i.e., corresponding to the growth conditions used in the present study) the density of large 2D clusters (with a lateral size from five up to several hundreds of nanometer) was measured to be $\approx 10^9$ cm⁻²,³⁰ implying that the centers of the adjacent localizing potentials are separated by ≈ 320 nm on the average.

It should be pointed out that the probabilities for electrons and holes to get localized at potential fluctuations are different. Holes in GaAs are ≈ 6.7 times heavier than electrons and consequently, if a particle has been captured into localizing potential at fixed sample temperature, the probability to remain localized is greater for holes compared to that for electrons. Localized holes and electrons can recombine radiatively in the localizing potentials, which are evidenced by the fine structure observed on the low-energy tail of the WL emission [see for example Fig. 1(a) of Ref. 32]. This circumstance together with the faster “cooling” rate for holes compared to that for electrons (as explained above) is responsible for the extra negative charge accumulated inside the single QD under study at zero external magnetic field (see Fig. 1).

Second, there is an internal built-in electric field (F) inside the structure with a component directed in the plane of the sample. The existence of such an internal electric field have been reported for QD samples based on different material compositions such as InAs/GaAs,^{32–35} CdSe/ZnSSe,³⁶ CdSe/ZnSe,³⁷ and InP/InGaP.³⁸ The origin of F is suggested to be due to ionized impurities spatially separated from the QD.^{36,37,39} The magnitude and direction of this internal field at a given time is determined by the charge distribution and distances between the impurities positioned in the close vicinity of the QD. In our previous papers,^{32,34,35} we investigated the influence of F on the carrier transport at $B=0$. The studies of single dots allowed us to estimate the time and space-averaged magnitude of this internal field to be 400 V cm⁻¹ in experiments with double-laser excitation at zero external electric field³² and 470 V cm⁻¹ when employ-

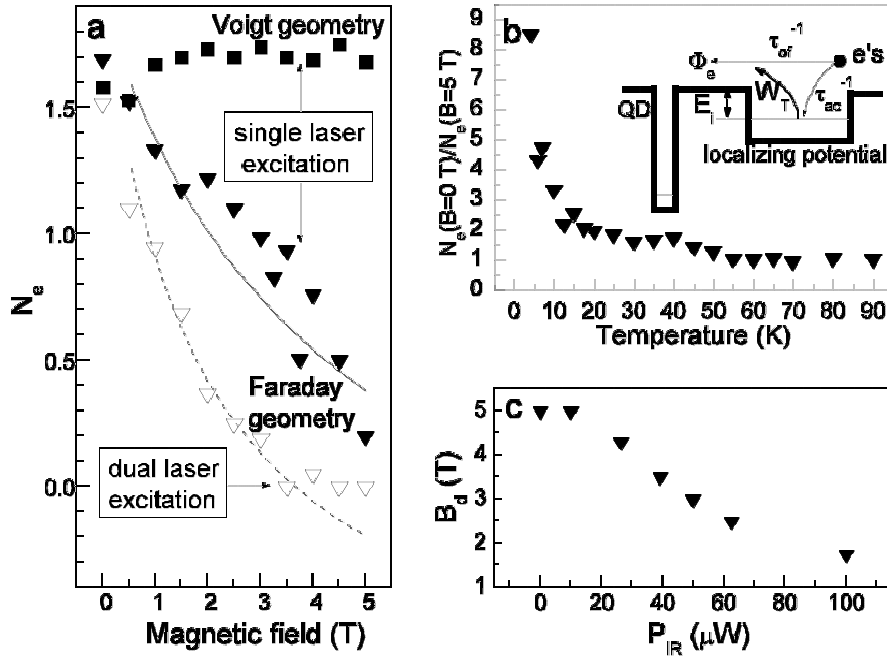


FIG. 2. (a) Number of extra electrons in QD (N_e) as a function of the magnetic field shown by solid (open) symbols for single-(dual) laser excitation conditions at $T=4.2$ K. The solid triangles (squares) correspond to the Faraday (Voigt) geometry. Data derived for single-laser excitation (solid triangles) are obtained from Fig. 1. The dual-laser data were recorded at $h\nu_{ex}=1.589$ eV, $P_0=20$ nW, $h\nu_{IR}=1.23$ eV, and $P_{IR}=50$ μW . The solid and dashed lines are fits to the data calculated on the basis of Eq. (1) as explained in the text. (b) Strength of the redistribution effect $N_e(B=0)/N_e(B=5 T)$ measured in the Faraday geometry at $h\nu_{ex}=1.540$ eV, $P_0=20$ nW, and for a number of temperatures. (c) Magnetic field at which $N_e \approx 0.2$ (B_d) as a function of P_{IR} measured in the Faraday geometry with dual-laser excitation at $T=4.2$ K, $h\nu_{ex}=1.589$ eV, $h\nu_{IR}=1.23$ eV, and $P_0=20$ nW. The inset in (b) is a schematic illustration of the assumed conduction-band profile of the sample including the QD and the localizing potential. The arrows indicate processes explained in the text.

ing single-laser excitation at nonzero external electric field.³⁴ From the studies of QDs ensembles in an external electric field at both single- and double-laser excitation conditions, $F=520$ V cm⁻¹ was obtained.³⁵ Accordingly, an internal field of $F \approx 500$ V cm⁻¹ is assumed at the single-laser excitation conditions.

The motion of electrons in the GaAs barriers prior to capture into the QD is affected by both localizing potentials and internal electric fields. At $B=0$ an electron is expected to possess a thermal velocity $v_T=(2k_B T/m_e)^{1/2}$, where k_B is the Boltzmann constant. The velocity that could be achieved in the presence of an electric field is $v_F=\mu^e \times F$. For low temperature (4.2 K) these velocities are calculated²⁸ to be $v_T=4.4 \times 10^6$ cm/s and $v_F=45 \times 10^6$ cm/s, respectively. At high magnetic fields, the kinetic energy of the carriers possessed at $B=0$ (in a direction perpendicular to the magnetic field) cancels and is quantized in the units of $\hbar\omega_c$.⁴⁰ If (in addition to the magnetic field) also an electric field is applied, perpendicularly to the direction of the magnetic field, a carrier will only be allowed to exhibit a motion with the drift velocity $V_{dr}=F/B$ directed perpendicular to both the electric and the magnetic fields.⁴¹ It is seen that at $B=5$ T $V_{dr}=1 \times 10^6$ cm/s, which is evidently less than both v_T and v_F . In other words, for the highest magnetic fields employed in our experiments, the motion of an electron is essentially slowed down compared to the case of $B=0$.

As a result, the “neutralization” of the charged QD (Fig. 1) is explained in terms of a magnetic-field-induced slowing down of the electron motion which—in turn—considerably

increases the probability for electrons to be captured into localizing potentials.

As explained above, an electron on its way toward the QD will pass the localizing potentials (with an averaged time of flight τ_{of}) into which it can be captured by emission of an acoustic phonon (with a characteristic time τ_{ac}) as schematically shown in the inset in Fig. 2(b). Hence, the probability for an electron to pass over the localizing potential, i.e., the magnitude of the electron flux (Φ_e) coming toward the QD [inset in Fig. 2(b)] is proportional to $\tau_{of}^{-1}/(\tau_{ac}^{-1} + \tau_{of}^{-1}) = 1/(\tau_{of}/\tau_{ac} + 1)$. Consequently, it is reasonable to expect that the longer τ_{of} is the higher probability for capturing an electron into the localizing potential. Hence, the stronger suppression of an electron flux toward the QD is predicted. At this stage, we disregard the possibility of thermal ionization of the trapped electrons out of the localizing potential [with the probability W_T as shown in the inset in Fig. 2(b)] because of the low temperature (4.2 K). The effect of increased temperature will be discussed below.

The typical value of τ_{of} could easily be estimated if the characteristic size of the localizing potential (L) was known. In our previous study of another piece of the same sample, the potential was evaluated to be $L=47$ nm.³⁴ Accordingly, at $B=0$, $\tau_{of}(0 T)=L/v_F=0.1$ ps and at $B=5$ T, $\tau_{of}(5 T)=L/V_{dr}=4.7$ ps. However, it is clear from the above that the different values of τ_{of} achieved for different magnetic fields could not lead to the observed changes in Φ_e if $\tau_{of}(B) \ll \tau_{ac}(B)$ for the magnetic-field range $0 < B < 5$ T. Consequently, an estimate of τ_{ac} is needed.

To evaluate the typical value of τ_{ac} in MBE-quality GaAs material, we adopt the carrier relaxation time $\tau_{rt}=80$ ps at $B=0$ as determined from temporal dynamics of the PL signal in a MBE-grown GaAs/AlGaAs quantum well of 17-nm thickness.⁴² The main contribution to the relaxation time originates from the emission of a cascade of acoustic phonons because emission of optical phonons in GaAs takes much shorter time.⁴³ Hence, we calculate $\tau_{ac}=\tau_{rt}/N_{ph}$, where N_{ph} is an averaged number of acoustic phonons emitted by the electron to release its kinetic energy E_e . To estimate N_{ph} , we note that an electron during its cooling process can emit acoustic phonon of energy $\hbar\omega_{ph}$ ranging from zero up to $\hbar\omega_{ph}^{max}=2v_l(2m_eE_e)^{1/2}-2m_ev_l^2$ as calculated considering an elementary act of the electron-phonon interaction (assuming a parabolic conduction band), where $v_l=5.2\times 10^5$ cm/s is the velocity of longitudinal-acoustic phonons in GaAs.⁴⁴ Thus, $\hbar\omega_{ph}^{max}=1.2$ meV for $E_e=19.2$ meV. Assuming averaged $\hbar\omega_{ph}\approx\hbar\omega_{ph}^{max}/2$, we conclude $N_{ph}\approx 30$ and, hence, $\tau_{ac}\approx 3$ ps, which is of the same order as $\tau_{of}(5$ T). It is important to note that with increasing magnetic field, τ_{rt} and, hence, τ_{ac} was found to exhibit a gradual increase (τ_{rt} was increased up to 120 ps at $B=5$ T).⁴² Thus, according to Ref. 42, with an increase of B from 0 up to 5 T, τ_{ac} increases by just a factor of 1.5 while $\tau_{of}(B)$ increases by 47 times for the same experimental conditions. As a result we can consider τ_{ac} to be independent of B .

Figure 2(a) shows the number of extra electrons (N_e) accumulated in the QD in its dependence on B . N_e was derived from experimental data of Fig. 1 on the basis of the following equation: $N_e=2\times W_2+W_1$, where $W_{1(2)}=I_X^{1-(2-)} / I_{QD}$. Here $I_X^{1-(2-)}$ is the spectrally integrated PL intensity of the X^{1-} (X^{2-}) PL lines and I_{QD} is the sum over all three PL lines in Fig. 1 (including X^0 PL line). It is seen that with increasing magnetic field, N_e progressively decreases to reach ≈ 0.2 at $B=5$ T [Fig. 2(a)]. The number of extra electrons accumulated in the QD is considered to be proportional to the difference between the fluxes of electrons (Φ_e) and holes (Φ_h). Assuming (as above) Φ_h to be unaffected by a magnetic field, N_e can be expressed in the following way:

$$N_e = \frac{\Phi_e - \Phi_h}{\Phi_h} = \frac{C}{\tau_{of}/\tau_{ac} + 1} - 1 = \frac{C}{\alpha \times B + 1} - 1, \quad (1)$$

where $\alpha=L/(\tau_{ac}\times F)$ and C are constants. A fit to the experimental data with Eq. (1) is shown in Fig. 2(a). It is seen that the fitting curve can reproduce the experimental data satisfactorily. From the fit, we find the parameter $\alpha=0.22$ T⁻¹ which, assuming $L=47$ nm and $F=500$ V cm⁻¹, results in $\tau_{ac}=4.3$ ps. This value is in a good agreement with the expected magnitude of $\tau_{ac}\approx 3$ ps as was estimated above. It should be mentioned that the lowest value of B used in the fitting procedure was restricted to 0.56 T providing $\omega_c^e \times \tau_{sc}^e \geq 1$.

It is interesting to note that our model [Eq. (1)] predicts that N_e should be entirely dependent on the ratio B/F . Consequently, if one increases (decreases) F , the same N_e should be achieved at the value of B , which increased (decreased) by the same amount. To check this idea, we decided to decrease the strength of the internal field F by an illumination of the sample with an additional infrared (IR) laser (see Ref.

35). The evolution of N_e versus B as obtained in experiments with dual-laser excitation conditions is shown in Fig. 2(a). It is evident that $N_e\approx 0.2$ has been reached already at $B=3$ T and, moreover, $N_e=0$ at $B\geq 3.5$ T. A fit to these data [Fig. 2(a)] was performed with the same value of C , which was derived from the fitting curve corresponding to single-laser excitation conditions. The parameter $\alpha=0.52$ T⁻¹ evaluated from this fit implies that in experiments with dual-laser excitation, the field F has decreased by a factor of 2.4 compared to single-laser excitation conditions. We further determined the value of B (B_d) at which $N_e\approx 0.2$ for a given excitation power of the IR laser (P_{IR}). The results are shown in Fig. 2(c). It is clear that B_d is progressively reduced with increasing P_{IR} (i.e., with decrease of F) in full agreement with Eq. (1). These experimental observations support the model proposed.

To further check the suggested model, we applied a magnetic field parallel to the sample surface (i.e., in the Voigt geometry). In this experimental arrangement, the magnetic field cannot totally quantize the in-plane motion of the electrons and, accordingly, the electron flux toward the QD should not be slowed down. In other words, N_e should remain almost the same at any magnetic field applied in the Voigt geometry. The corresponding data are shown in Fig. 2(a). Indeed, N_e remains almost constant (with a slight increase from 1.6 up to 1.7 with an increasing magnetic field from 0 up to 5 T) with respect to the case of Faraday geometry [Fig. 2(a)]. This experimental observation also supports the suggested model.

To finally check the developed model, the temperature (T) evolution of the observed phenomenon was studied. Our model is based on the magnetic-field-induced localization of electrons on the heterointerface potentials. Evidently, at elevated temperatures, thermal ionization with increase of T will increase with a probability W_T proportional to $(\exp\{E_i/k_B T\}-1)^{-1}$, where E_i is the ionization energy of localized electron. These processes are schematically shown by the arrow marked with W_T in the inset in Fig. 2(b). As a result, a more limited influence of a magnetic field on the electron flux is expected as the temperature is elevated. Corresponding data in terms of the strength of the redistribution effect defined as $N_e(B=0)/N_e(B=5$ T) for a number of temperatures are shown in Fig. 2(b). It is evident that the strength of the redistribution effect progressively decreases from 8.5 (at $T=4.2$ K) down to 1 (at $T\geq 55$ K), which supports the suggested model. The rate of the observed decrease is fast in the temperature range from 4.2 to 10 K implying that E_i should be of the order of 1 meV. This value is in reasonable agreement⁴⁵ with an averaged value of ionization energy found for holes (≈ 2.8 meV) in our previous work,³⁴ where we studied another piece of the same sample in an external electric field.

IV. CONCLUSIONS

In conclusion, a magnetic-field-induced charging control of individual QDs has been obtained. At above barrier photoexcitation, the population of the QD with excess e^- 's is modified with an external magnetic field in Faraday geom-

etry that controls the electron transport in the QD plane. The field strength required to control the charging is dot dependent and it can also be tuned by using an additional infrared excitation source. Temperature dependence measurements support the proposed explanation. The reported redistribution effect can be used as a nondestructive tool to estimate the magnitude of the in-plane electric field around a QD.

ACKNOWLEDGMENTS

This work was supported by grants from the Swedish Foundation for Strategic Research (SSF) and the Swedish Research Council (VR). E.S.M. gratefully acknowledges the financial support from the Royal Swedish Academy of Sciences (KVA).

- ¹L. Harris, D. J. Mawbray, M. S. Skolnick, M. Hopkinson, and G. Hill, *Appl. Phys. Lett.* **73**, 969 (1998).
- ²T. Lundstrom, W. Schoenfeld, H. Lee, and P. M. Petroff, *Science* **286**, 2312 (1999).
- ³D. Bimberg, M. Grundmann, and N. N. Ledentsov, *Quantum Dot Heterostructures* (Wiley, London, 1999).
- ⁴D. V. Regelman, E. Dekel, D. Gershoni, E. Ehrenfreund, A. J. Williamson, J. Shumway, A. Zunger, W. V. Schoenfeld, and P. M. Petroff, *Phys. Rev. B* **64**, 165301 (2001).
- ⁵I. A. Yugova, A. Greilich, E. A. Zhukov, D. R. Yakovlev, M. Bayer, D. Reuter, and A. D. Wieck, *Phys. Rev. B* **75**, 195325 (2007).
- ⁶A. Hartmann, Y. Ducommun, E. Kapon, U. Hohenester, and E. Molinari, *Phys. Rev. Lett.* **84**, 5648 (2000).
- ⁷E. S. Moskalenko, K. F. Karlsson, P. O. Holtz, B. Monemar, W. V. Schoenfeld, J. M. Garcia, and P. M. Petroff, *Phys. Rev. B* **66**, 195332 (2002).
- ⁸R. J. Warburton, C. Schaflein, F. Haft, F. Bickel, A. Lorke, K. Karrai, J. M. Garcia, W. Schoenfeld, and P. M. Petroff, *Nature (London)* **405**, 926 (2000).
- ⁹M. Baier, F. Findeis, A. Zrenner, M. Bichler, and G. Abstreiter, *Phys. Rev. B* **64**, 195326 (2001).
- ¹⁰M. Sugisaki, H. W. Ren, S. V. Nair, K. Nishi, and Y. Masumoto, *Phys. Rev. B* **66**, 235309 (2002).
- ¹¹D. Hessman, J. Persson, M. E. Pistol, C. Pryor, and L. Samuelson, *Phys. Rev. B* **64**, 233308 (2001).
- ¹²Y. Igarashi, M. Jung, M. Yamamoto, A. Oiwa, T. Machida, K. Hirakawa, and S. Tarucha, *Phys. Rev. B* **76**, 081303(R) (2007).
- ¹³X. Xu, Y. Wu, B. Sun, Q. Huang, J. Cheng, D. G. Steel, A. S. Bracker, D. Gammon, C. Emary, and L. J. Sham, *Phys. Rev. Lett.* **99**, 097401 (2007).
- ¹⁴T. Nakaoka, S. Tarucha, and Y. Arakawa, *Phys. Rev. B* **76**, 041301(R) (2007).
- ¹⁵A. S. Bracker, E. A. Stinaff, D. Gammon, M. E. Ware, J. G. Tischler, A. Shabaev, A. L. Efros, D. Park, D. Gershoni, V. L. Korenev, and I. A. Merkulov, *Phys. Rev. Lett.* **94**, 047402 (2005).
- ¹⁶W. H. Chang, W. Y. Chen, M. C. Cheng, C. Y. Lai, T. M. Hsu, N. T. Yeh, and J. I. Chyi, *Phys. Rev. B* **64**, 125315 (2001).
- ¹⁷J. G. Tischler, A. S. Bracker, D. Gammon, and D. Park, *Phys. Rev. B* **66**, 081310(R) (2002).
- ¹⁸J. J. Finley, D. J. Mowbray, M. S. Skolnick, A. D. Ashmore, C. Baker, A. F. G. Monte, and M. Hopkinson, *Phys. Rev. B* **66**, 153316 (2002).
- ¹⁹G. Ortner, M. Bayer, A. Larionov, V. B. Timofeev, A. Forchel, Y. B. Lyanda-Geller, T. L. Reinecke, P. Hawrylak, S. Fafard, and Z. Wasilewski, *Phys. Rev. Lett.* **90**, 086404 (2003).
- ²⁰T. Flissikowski, I. A. Akimov, A. Hundt, and F. Henneberger, *Phys. Rev. B* **68**, 161309(R) (2003).
- ²¹M. Bayer, G. Ortner, O. Stern, A. Kuther, A. A. Gorbunov, A. Forchel, P. Hawrylak, S. Fafard, K. Hinzer, T. L. Reinecke, S. N. Walck, J. P. Reithmaier, F. Klopff, and F. Schäfer, *Phys. Rev. B* **65**, 195315 (2002).
- ²²M. Larsson, E. S. Moskalenko, L. A. Larsson, P. O. Holtz, C. Verdozzi, C.-O. Almbladh, W. V. Schoenfeld, and P. M. Petroff, *Phys. Rev. B* **74**, 245312 (2006).
- ²³E. S. Moskalenko, K. F. Karlsson, P. O. Holtz, B. Monemar, W. V. Schoenfeld, J. M. Garcia, and P. M. Petroff, *Phys. Rev. B* **64**, 085302 (2001).
- ²⁴H. Hillmer, A. Forchel, S. Hansmann, M. Morohashi, E. Lopez, H. P. Meier, and K. Ploog, *Phys. Rev. B* **39**, 10901 (1989).
- ²⁵C. Kittel, *Introduction to Solid State Physics*, 5th ed. (Wiley, New York, 1976).
- ²⁶C. M. Wolfe, G. E. Stillman, and W. T. Lindley, *J. Appl. Phys.* **41**, 3088 (1970).
- ²⁷D. E. Hill, *J. Appl. Phys.* **41**, 1815 (1970).
- ²⁸It should be noted that for the case of electrons, experimental data on mobility are available for temperatures down to 4.2 K (Ref. 26), while for the case of holes the lowest temperature is 20 K (Ref. 27). To extract μ^h at $T=4.2$ K, we used the following procedure: First, on the basis of formulas given in Ref. 26, μ^h was calculated for $T=20$ K. It was found to differ by only 30% compared to μ^h measured in Ref. 27 at $T=20$ K. Second, we calculated $\mu^h=2\,970$ cm²/Vs for $T=4.2$ K and compared this value with $\mu^e=90\,000$ cm²/Vs, as was measured at $T=4.2$ K (Ref. 26) (i.e. μ^e is larger than μ^h by a factor of >30). It is important to note that the ratio μ^e/μ^h obtained from the experiments (Refs. 26 and 27) at $T=20$ K is ≈ 28 . As a result, we consider $\mu^h\approx 3\,000$ cm²/Vs as a good approximation at $T=4.2$ K.
- ²⁹C. Lobo, R. Leon, S. Marcinkevicius, W. Yang, P. C. Sercel, X. Z. Liao, J. Zou, and D. J. H. Cockayne, *Phys. Rev. B* **60**, 16647 (1999).
- ³⁰R. Heitz, T. R. Ramachandran, A. Kalburge, Q. Xie, I. Mukhametzhanov, P. Chen, and A. Madhukar, *Phys. Rev. Lett.* **78**, 4071 (1997).
- ³¹T. J. Krzyzewski, P. B. Joyce, G. R. Bell, and T. S. Jones, *Phys. Rev. B* **66**, 121307(R) (2002).
- ³²E. S. Moskalenko, V. Donchev, K. F. Karlsson, P. O. Holtz, B. Monemar, W. V. Schoenfeld, J. M. Garcia, and P. M. Petroff, *Phys. Rev. B* **68**, 155317 (2003).
- ³³P. W. Fry, J. J. Finley, L. R. Wilson, A. Lemaître, D. J. Mowbray, M. S. Skolnick, M. Hopkinson, G. Hill, and J. C. Clark, *Appl. Phys. Lett.* **77**, 4344 (2000).
- ³⁴E. S. Moskalenko, M. Larsson, W. V. Schoenfeld, P. M. Petroff, and P. O. Holtz, *Phys. Rev. B* **73**, 155336 (2006).

- ³⁵E. S. Moskalenko, M. Larsson, K. F. Karlsson, P. O. Holtz, B. Monemar, W. V. Schoenfeld, and P. M. Petroff, *Nano Lett.* **7**, 188 (2007).
- ³⁶V. Türck, S. Rodt, O. Stier, R. Heitz, R. Engelhardt, U. W. Pohl, D. Bimberg, and R. Steingrüber, *Phys. Rev. B* **61**, 9944 (2000).
- ³⁷R. G. Neuhauser, K. T. Shimizu, W. K. Woo, S. A. Emedocles, and M. G. Bawendi, *Phys. Rev. Lett.* **85**, 3301 (2000).
- ³⁸V. Davydov, I. Ignatiev, H. W. Ren, S. Sugou, and Y. Masumoto, *Appl. Phys. Lett.* **74**, 3002 (1999).
- ³⁹M. Sugisaki, H. W. Ren, K. Nishi, and Y. Masumoto, *Phys. Rev. Lett.* **86**, 4883 (2001); H. D. Robinson and B. B. Goldberg, *Phys. Rev. B* **61**, R5086 (2000).
- ⁴⁰G. F. Giuliani and G. Vignali, *Quantum Theory of the Electron Liquid* (Cambridge University Press, Cambridge, 2005).
- ⁴¹This is valid in both classical (Ref. 25) and quantum-mechanical (Ref. 40) approaches.
- ⁴²I. Aksenov, Y. Aoyagi, J. Kusano, T. Sugano, T. Yasuda, and Y. Segawa, *Phys. Rev. B* **52**, 17430 (1995).
- ⁴³H. W. Yoon, D. R. Wake, and J. P. Wolfe, *Phys. Rev. B* **54**, 2763 (1996).
- ⁴⁴K. Lee, M. S. Shur, T. J. Drummond, and H. Morkoç, *J. Appl. Phys.* **54**, 6432 (1983).
- ⁴⁵As holes in GaAs are ≈ 6.7 times heavier than electrons, it is reasonable to assume that holes should have less quantization energy inside the localizing potential and, hence, larger ionization energy compared to that for electrons.